Journal of
Synchrotron Radiation

ISSN 0909-0495

Received 21 November 2005
Accepted 19 September 2006

EXAFS characterization of oxaliplatin anticancer drug and its degradation in chloride media

Diane Bouvet,[a]* Alain Michalowicz,[a] Sylvie Crauste-Manciet,[b,c] Emmanuel Curis,[d] Ioannis Nicolis,[d] Luca Olivi,[e] Gilberto Vlaic,[e,f] Denis Brossard[b,c] and Karine Provost[a]

[a]Laboratoire de Physique Structurale des Molécules et Matériaux, Université Paris XII, 61 avenue du Général De Gaulle, 94010 Créteil CEDEX, France, [b]Laboratoire de Pharmacie Galénique, Université Paris V, 75006 Paris, France, [c]Service de Pharmacie, CHI Poissy Saint Germain en Laye, 78105 Saint Germain en Laye, France, [d]Laboratoire de Biomathématiques, Faculté de Pharmacie, Université Paris V, 75006 Paris, France, [e]ELETTRA Sincrotrone Trieste SCpA, Italy, and [f]Department of Chemical Science, University of Trieste, Italy. E-mail: bouvet@univ-paris12.fr

Oxaliplatin is a second-generation platinum-based anticancer drug. Its degradation is studied in solution, in the presence of chloride ions (in neutral or acidic media) in excess. In both cases the degradation product precipitates immediately. The EXAFS spectra of these products show that they are identical. EXAFS modeling and refinement of the first coordination sphere shows that two light atoms are replaced by two chloride ions. The complete refinement of the local structure is possible by studying the multiple-scattering signal. The results show that the main multiple-scattering contribution is due to the binding oxalato group and that the degradation product is [Cl_2-(diaminocyclohexane)-Pt(II)].

Keywords: oxaliplatin; platinum antitumoral drugs; EXAFS structure; multiple scattering; solution stability.

1. Introduction

Platinum (II) complexes are largely used for antitumoral therapy. Among them, carboplatin and oxaliplatin are second-generation drugs belonging to the cisplatin structural family. Oxaliplatin [oxalato(*trans-l*-1,2-diaminocyclohexane)platinum II)] has demonstrated a broad spectrum of antitumor activity, and is used in colorectal carcinoma treatment (Chollet *et al.*, 1996; Wiseman *et al.*, 1999; Lokich, 2001).

The critical role of DNA-Pt adducts in antiproliferative effects, well documented for cisplatin, is generally accepted for all antitumor Pt drugs (Sanderson *et al.*, 1996). Models of oxaliplatin-induced DNA lesions are largely based on an extrapolation of results that are well established for cisplatin and diaminocyclohexane (DACH) compounds other than oxaliplatin. Oxaliplatin is typically at least as potent as cisplatin in inhibiting the growth of cancer cells (Rixe *et al.*, 1996). The structures of DACH–Pt-DNA adducts formed by oxaliplatin and *cis*-diamine–Pt-DNA adducts (formed by cisplatin) seem to be similar, but the bulky DACH moiety that protrudes into the minor groove may possibly lead to different biological properties of the adducts (Scheeff *et al.*, 1999).

The stability of carboplatin in the presence of chloride ions, provided under perfusion conditions, has been largely studied (Benaji *et al.*, 1994; Valiere *et al.*, 1996; Lederer & Leipzig-Pagani, 1998). The reaction has been shown to produce cisplatin (Curis *et al.*, 2000), which increases the drug toxicity. Such a degradation may also occur in the case of oxaliplatin.

In a preliminary study, our results have shown a progressive degradation of oxaliplatin under well defined chloride concentration and pH conditions (Curis *et al.*, 2001). However, the study was only qualitative without any structural modeling beyond the first coordination sphere. To our knowledge there is, as yet, no other structural study of this degradation of oxaliplatin. In this paper we consider the behavior of oxaliplatin in the presence of hydrochloric acid and sodium chloride. The degradation products are obtained as precipitates. The present X-ray absorption (EXAFS) study of known Pt(II) oxalate complexes proves that this method is able to discriminate efficiently between the binding of each type of ligand to the platinum center, if the EXAFS modeling is extended to the outer shells, including multiple-scattering contributions. Following the method employed for the model compounds, it was possible to model completely the structure of the unknown complexes obtained by the reaction of oxaliplatin in the presence of chloride ions in solution.

2. Experiments and data analysis

2.1. Sample preparation

Powdered $Pt(ox)_2$ was purchased from Aldrich. Powdered oxaliplatin was obtained from a Sanofi pharmaceutical preparation, diluted to 10 mg ml^{-1} (25 m*M*) for the solution experiments. In the hydrochloric acid solution, final concentrations were 2.2 *M* in HCl and 20 m*M* in oxaliplatin. For the sodium chloride solution, final concentrations were 3.7 *M* in NaCl and 25 m*M* in oxaliplatin. Thus chloride ions were largely in excess and the reaction was expected to be as complete as possible.

Both solutions with HCl and NaCl precipitated immediately under these conditions. The precipitates were washed in water, separated by centrifugation, and oven dried before XAS measurement. The XAFS spectra of the supernatant liquid do not show any Pt(II) L_{III}-edge jump within the error bars. This proved that more than 99% of platinum had precipitated. Model compounds and precipitates solid samples were prepared as a homogenous mixture of pure product and cellulose compressed pellets. The quantity of product was calculated in order to obtain an edge jump $\Delta\mu x$ near to 1, with a total absorbance after the edge $\mu x(E) < 2$.

2.2. XAS measurements and analysis

Oxaliplatin, $Pt(ox)_2$ and the precipitate with hydrochloric acid spectra were recorded in transmission mode at LURE (the French synchrotron radiation facility) on the EXAFS13 station of the storage-ring DCI, with the following experimental conditions: Pt L_{III}-edge, Si(111) channel-cut monochromator, 11450–12600 eV energy range. The precipitate with sodium chloride spectrum was recorded at ELETTRA on station BL11.1, with the following experimental conditions: Pt L_{III}-edge, Si(111) double-crystal monochromator, 11260–13000 eV energy range. The spectra were extracted using standard procedures (Teo, 1986; Koenigsberger & Prins, 1988; Lytle *et al.*, 1989) available in the program *EXAFS pour le Mac* (Michalowicz, 1997), including spline-smoothing atomic absorption determination, energy-dependent normalization and fast Fourier transform (E_0 = 11560 eV, Fourier transform range 2–12 Å). Each spectrum was recorded three times and averaged.

EXAFS modeling of the complete structures was performed in three steps:

(i) Fourier filtering of the main peak and fitting of the EXAFS contribution from the neighbors directly bound to platinum. This preliminary fit has two aims: to determine the type and number of atoms directly bonded to the Pt(II) ion, and to verify that the fitted platinum–ligand distance is coherent with known distances found in the literature.

(ii) Construction of the molecular models using the program *Chem3D* using crystallographic structures when they are known, or characteristic crystallographic distances and knowledge of the ligands structures. Preparation of the resulting *FEFF* (Rehr *et al.*, 1992) input files using the code *CRYSTALFF* (Provost *et al.*, 2001).

(iii) *Ab initio* EXAFS modeling with *FEFF7*. Sorting of the most important single- and multiple-scattering paths. Equivalent paths are grouped in order to fit with a single amplitude–phase function. For model compounds the fit result is compared with known crystal structures (Mattes & Krogmann, 1964; Bruck *et al.*, 1984). For the unknown compounds, several models of ligand binding are tested and quantitatively compared using the statistical F-test (Joyner *et al.*, 1987; Michalowicz *et al.*, 1999).

All the fits of steps (i) and iii) were performed using the *Round Midnight* code (Michalowicz, 1997) by comparing the experimental spectra with the standard EXAFS formula including single- and multiple-scattering paths (Rehr *et al.*, 1992).

Amplitude and phase functions were calculated using the *FEFF7* code. Since theoretical phase shifts and amplitudes were used, it was necessary to fit the energy threshold E_0. The photoelectron mean free path was set to the empirical minimal curve (Teo, 1986).

Optimal values for Γ and η were fitted for the two model compounds $Pt(ox)_2$ and oxaliplatin, and finally set to $\eta = 3.1$ and $\Gamma = 0.7$. In the modeling of the filtered first coordination sphere we fitted separated Debye–Waller (DW) factors σ_i for each type of atom. For the fit of the complete spectra it was necessary to limit the total number of fitted parameters in order to limit the correlations and improve the fitting statistics. Thus it was decided to fit a global DW factor for all of the shells. In all cases a global ΔE_0 was refined.

The goodness of fit, or quality factor, is QF = $\Delta\chi_{min}{}^2/\nu$, where $\Delta\chi_{min}$ is the minimum value of the statistical $\Delta\chi^2_{stat}$ [equation (1)], and the degree of freedom $\nu = N_{ind} - N_{par}$, where N_{ind} is the number of independent points and N_{par} is the total number of fitted parameters,

$$\Delta\chi^2_{stat} = \frac{N_{ind}}{N_{pt}} \sum_i \left[k\chi_{th}(i) - k\chi_{exp}(i)\right]^2/\varepsilon_i^2. \qquad (1)$$

Here, N_{pt} is the number of experimental points and ε_i^2 is the experimental error. Statistical errors on the average spectra and error bars of the fitted parameters are evaluated as recommended by the IXS Standard and Criteria subcommittee (report 2000, http://ixs.iit.edu/subcommittee_reports/sc/).

The EXAFS spectra were fitted in the range 3–12 $Å^{-1}$. The *R*-space fitted range was 0–2.5 Å for the first-shell fits and 0–5 Å for the complete spectra. The number of independent points, $N_{ind} = 2\Delta k\,\Delta R/\pi$, was 14 and 28, respectively. The average experimental error was evaluated as $\langle\varepsilon\rangle = 0.015$.

3. Results and discussion

3.1. Experimental spectra

The experimental signals of the four samples are presented in Fig. 1. $Pt(oxalate)_2$ (Fig. 1*a*) and oxaliplatin (Fig. 1*b*) are the two model compounds. Figs. 1(*c*) and 1(*d*) represent the EXAFS spectra of the reaction products between oxaliplatin and two chloride species in excess: hydrochloric acid and

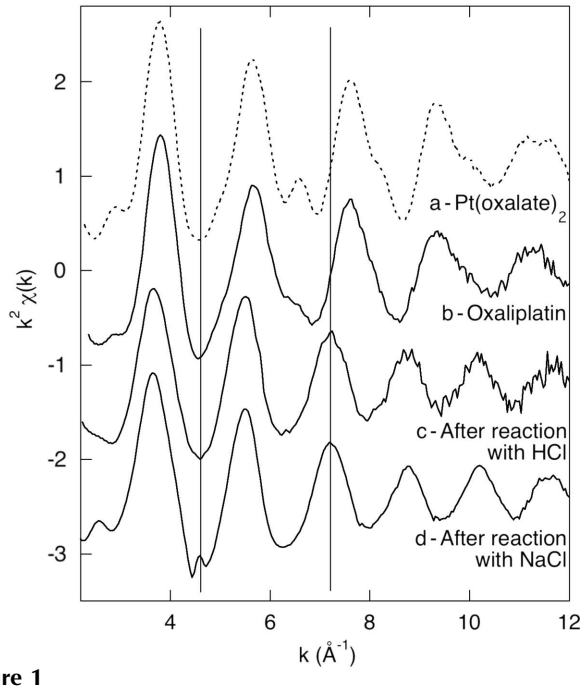

Figure 1
EXAFS spectra of $Pt(oxalate)_2$, oxaliplatin, and oxaliplatin after reaction with two reactants: hydrochloric acid and sodium chloride.

sodium chloride, respectively. The corresponding Fourier transforms (without phase-shift correction) are presented in Fig. 2.

As shown in Fig. 3, the structure of $Pt(II)(ox)_2$ is composed of two oxalate ligands chelating the central Pt(II) ion by four Pt—O bonds. In oxaliplatin, one oxalate is replaced by a diaminocyclohexane (DACH) ligand, bonded by two N atoms. The EXAFS spectra Fourier transforms of these two model compounds are consistent with their structures. The Fourier transform of the $Pt(ox)_2$ spectrum presents three main peaks at structural distances: the four Pt—O bonds at 2.01 Å for the first peak, and the four Pt—C distances at 2.77 Å for the second. As the crystallographic structure of $Pt(ox)_2$ (Mattes & Krogmann, 1964) presents a quasi-alignment of the PtCO′ atoms, the third peak may be related to multiple scattering through the carbonyl groups of oxalate.

The Fourier transform of oxaliplatin is similar to that of $Pt(ox)_2$, except for the third peak which is significantly decreased. This feature confirms that the main contribution of this peak is due to the outer O atoms of the oxalate ligand. This qualitative discussion will be confirmed quantitatively in the modeling section.

The spectra of the two degradation products with chloride ions are identical within the error bars, suggesting that the resulting precipitate is independent of the reagent (HCl or NaCl). The EXAFS spectra of these products are drastically different from that of oxaliplatin, suggesting a huge change in the structure. The first peak, corresponding to the directly bonded atoms, is largely modified (Figs. 2*c* and 2*d*). The first shell seems to be split into two different contributions, as expected for an important Pt(II)–ligand bonding modification. At least, the multiple-scattering outer-shell signal is significantly decreased. These features are proof that oxaliplatin is converted into a unique degradation product in the presence of Cl^- ions.

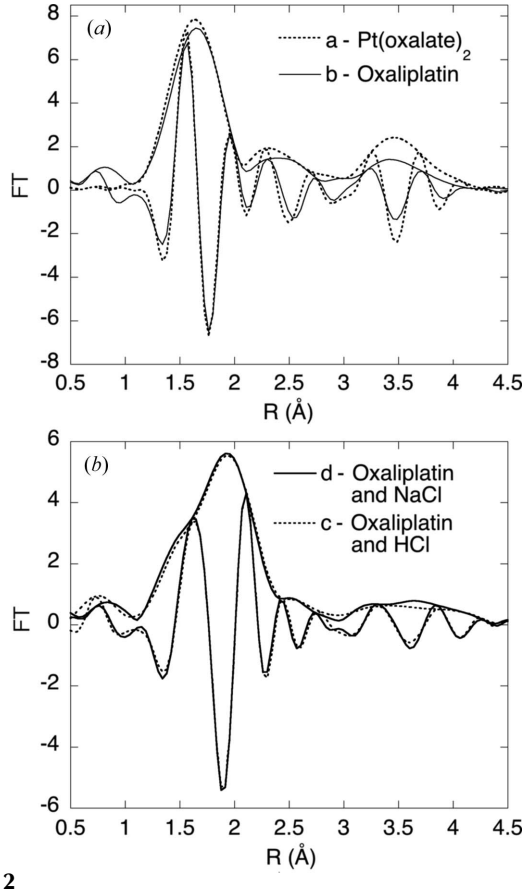

Figure 2
Fourier transform (FT) modules and imaginary parts of $Pt(oxalate)_2$, oxaliplatin, and oxaliplatin after reaction with two reactants: hydrochloric acid and sodium chloride.

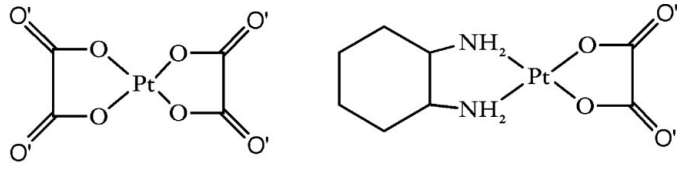

Figure 3
Formulae of $Pt(oxalate)_2$ (left) and oxaliplatin (right).

3.2. Modeling

3.2.1. $Pt(oxalate)_2$ model compound. The first-shell filtered spectrum was simulated by using four identical components (four O atoms). The number N of atoms in the shell was fixed, as were the DW factor σ and bond length R. The parameters of this simulation are presented in Table 1. The refined distance value is close to the crystallographic one (Mattes & Krogmann, 1964; Bruck *et al.*, 1984). The first multiple-scattering model of $Pt(ox)_2$ was proposed by Teo (1981), in the frame of the early plane-wave approximation.

In the present work the complete EXAFS spectrum of $Pt(ox)_2$ could be modeled *ab initio* up to 4 Å from the crys-

Table 1
Fit parameters of the first coordination shell for the two model compounds.

Path	N	$\sigma \times 10^2$ (Å)	R (Å)	R_{XR} (Å)
$Pt(oxalate)_2$				
Pt–O	4	5.0 (6)	1.99 (1)	R_a = 2.01
Residual = 4.66 × 10^{-2}, N_{par} = 3, QF = 3.41, ΔE = 10.3 (9) eV				
Oxaliplatin				
Pt–O/N	4	5.7 (6)	1.99 (1)	R_a = 2.03
Residual = 6.32 × 10^{-2}, N_{par} = 3, QF = 5.24, ΔE = 10.7 (4) eV				

Table 2
Fit parameters of the model compounds.

Path	N	$\sigma \times 10^2$ (Å)	R (Å)	R_{XR} (Å)
$Pt(oxalate)_2$ (Mattes & Krogmann, 1964)				
Pt–O	4	5.1 (3)	1.99 (1)	R_a = 2.01
Pt–C	4	5.1 (3)	2.77 (1)	R_b = 2.77
Pt–C–O′	4	5.1 (3)	3.97 (1)	R_c = 3.99
Pt–O–Pt–O	4	5.1 (3)	4.00 (2)	R_d = 4.02
Residual = 2.40 × 10^{-2}, N_{par} = 6, QF = 1.09, ΔE = 10.6 (2) eV				
Oxaliplatin (Bruck *et al.*, 1984)				
Pt–O/N	4	5.8 (7)	2.00 (1)	R_a = 2.03
Pt–C	4	5.8 (7)	2.82 (2)	R_b = 2.83
Pt–C–O′	2	5.8 (7)	4.00 (3)	R_c = 4.00
Pt–O–Pt–N	4	5.8 (7)	3.91 (3)	R_d = 4.06
Residual = 3.44 × 10^{-2}, N_{par} = 6, QF = 1.32, ΔE = 12.4 (5) eV				

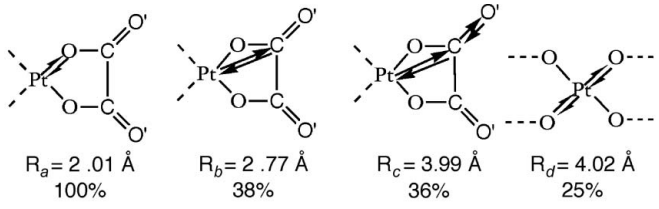

Figure 4
Most important scattering paths of the $Pt(ox)_2$ EXAFS signal. The *FEFF* amplitude ratio is given for each effective distance.

tallographic data using *FEFF7* in the frame of the spherical-wave approximation. Analysis of the most important scattering paths contributions showed that it was possible to limit the refinement of the platinum neighborhood to four groups of paths, as shown in Fig. 4. The first two groups correspond to simple scattering paths Pt–O and Pt–C with a degeneracy equal to 4 for each group. The third group takes into account the scattering paths concerning PtCO′ atoms where O′ is the outer oxygen of the oxalate ion. In the latter, we used multiple-scattering paths through the platinum.

Parameters of the best fit are presented in Table 2. The average distances obtained for each group are in good agreement with crystallographic data. All other parameters present acceptable values.

Fig. 5 presents a comparison between experimental and refined *FEFF*-simulated EXAFS spectra of $Pt(ox)_2$, and their respective Fourier transforms. The four-shell model detailed above correctly fits the complete EXAFS spectrum. We note that scattering through the carbonyl group dominates (36% *versus* 25% for the scattering through the platinum central atom). Nevertheless, according to the F-test (Michalowicz *et al.*, 1999), adding the scattering contribution through the central atom in the model improved it with a 99% probability.

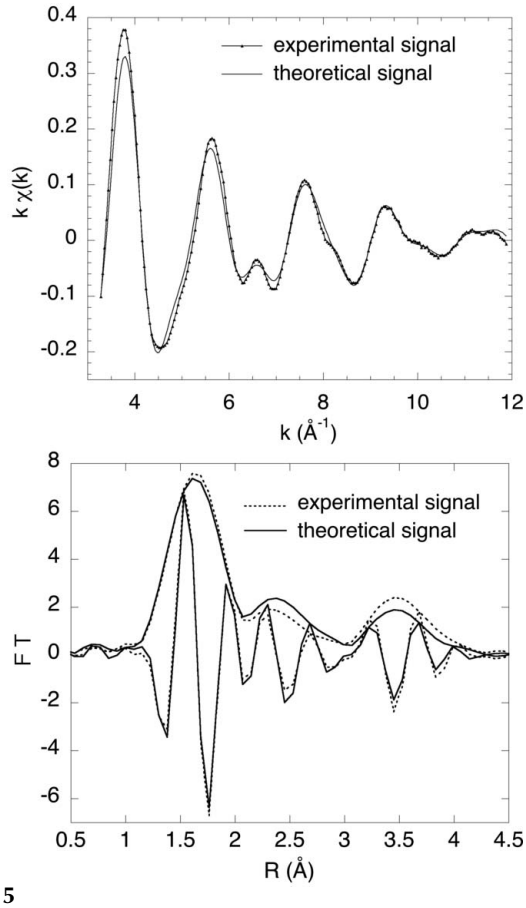

Figure 5
Comparison between experimental and simulated spectra of $Pt(ox)_2$: EXAFS (top) and Fourier transform amplitudes and imaginary parts (bottom).

3.2.2. Oxaliplatin model compound. A similar approach was performed for the EXAFS spectrum modeling of oxaliplatin. Since the PtN and PtO EXAFS single-scattering contributions cannot be distinguished, the filtered signal of the first platinum coordination shell was modeled using a single shell composed of four light atoms, four N/O. As in the case of $Pt(ox)_2$, the first-shell distances obtained in the best fit are in good agreement with crystallographic data (Bruck *et al.*, 1984) (Table 1).

The *ab initio FEFF* calculation of the EXAFS spectrum of oxaliplatin reveals many similarities and some differences from the *FEFF* model of the $Pt(ox)_2$ described above. In both models the main contributions are (i) four single-scattering PtN/O paths; (ii) four single-scattering PtC paths; (iii) all scattering paths implying PtCO′ atoms of the oxalate ligand; and (iv) multiple scattering through the platinum ion (Fig. 6). However, the degeneracy of the PtCO′ contribution is 2 instead of 4 for $Pt(ox)_2$, and it appears that the scattering contribution of the DACH ligand beyond the two first shells can be neglected, since their amplitudes do not exceed 10%.

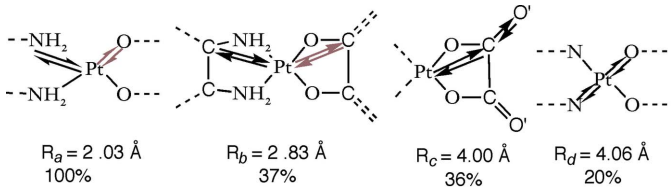

Figure 6
Most important scattering paths of the oxaliplatin EXAFS signal.

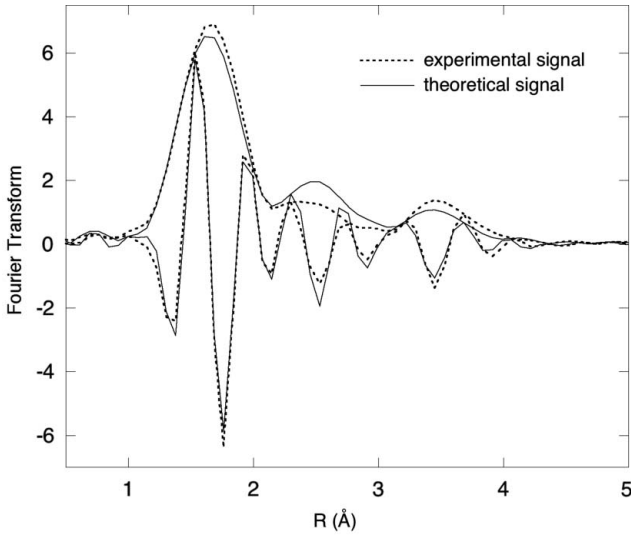

Figure 7
Comparison between experimental and simulated spectra (Fourier transform modules and imaginary parts) of oxaliplatin.

The best simulation parameters are presented in Table 2. As in the case of $Pt(ox)_2$, the complete model distances are in good agreement with the crystallographic data (Bruck *et al.*, 1984), even if the last distance (Pt–N–Pt–O) is slightly underestimated. With such parameters, the EXAFS spectrum and its Fourier transform are well reproduced (Fig. 7). Taking into account the multiple scattering through the central atom improves the model with a 74% probability.

Since the principal aim of this work was to characterize the structure of the degradation product of oxaliplatin in the presence of Cl^- ions, it is important to qualify precisely the ability of EXAFS to detect which ligand is actually displaced. As quoted above, we have shown that the outer contributions of DACH can be neglected. On the other hand, the signal around 4 Å observed in both model compounds is composed of two contributions: (i) multiple scattering through the aligned PtCO′ atoms of the oxalate carbonyl groups, and (ii) multiple scattering through the central Pt(II) ion. We have already shown that the first contribution dominates, even if the second cannot be totally neglected. This is illustrated in Fig. 8 where we have plotted the Fourier transform amplitudes of these various contributions calculated using *FEFF* under three different structural configurations (Fig. 9). For the three models the theoretical signals were calculated using a DW factor of 5.3×10^{-2} Å and $\Delta E = 10$ eV (these values are close to those obtained in both simulations), and then compared with the experimental spectrum.

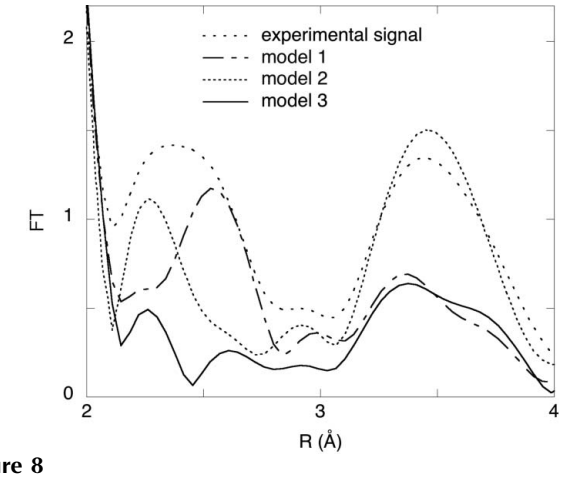

Figure 8
Comparison between the oxaliplatin signal and the three simulated signals. Fourier transform modules (zoom on the range 2–4 Å).

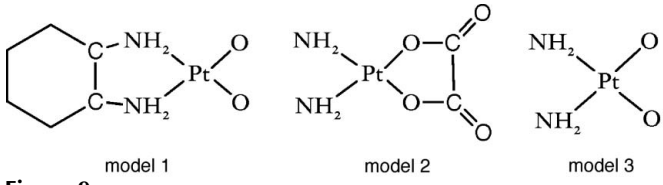

Figure 9
The three models used to determine the contribution of both ligands.

Model 1 corresponds to the whole first coordination sphere, the total mean and large distance DACH contribution and the multiple scattering though the central atom, assuming that the oxalate group contribution beyond the first coordination sphere is neglected. Model 2 represents the opposite model, which takes into account the total contribution of the outer shell of oxalate, and neglects the DACH contribution. The third model is calculated in order to evaluate the contribution of the first coordination sphere and the multiple-scattering paths through Pt(II).

In these three simulations the first Fourier transform peaks corresponding to the first coordination sphere are perfectly superimposed, as expected (data not shown). Nevertheless, these theoretical models show that the exceptional amplitude of the carbonyl signal, owing to the quasi-alignment (PtCO′ = 9.5°) of the three atoms in the oxaliplatin structure, is a signature of the oxalato ligand binding. In the case of a displacement of oxalate, the peak should be drastically decreased; in the case of a displacement of the DACH ligand, it should remain. It is thus possible to determine which ligand of oxaliplatin is actually displaced.

3.3. Degradation of oxaliplatin in the presence of Cl^- ions

As quoted in §3.1, the coordination sphere of oxaliplatin is drastically modified upon degradation by Cl^-. Fitting of the first coordination sphere was possible only with two light atoms (O or N) and two chloride ligands, as shown in Table 3. This model is coherent with the Pt—O and Pt—Cl distances found in the literature on known crystal structures (Milburn &

Table 3
Fit parameters of the first coordination shell for the two precipitates.

Path	N	$\sigma \times 10^2$ (Å)	R (Å)	R_{XR} (Å)
Oxaliplatin + NaCl precipitate				
Pt–N/O	2	5 (1)	2.00 (1)	R_e = 2.02
Pt–Cl	2	5.6 (4)	2.30 (1)	R_e = 2.31
Residual = 1.54×10^{-2}, N_{par} = 5, QF = 0.73, ΔE = 5.9 (6) eV				
Oxaliplatin + HCl precipitate				
Pt–N/O	2	5.3 (8)	2.00 (1)	R_e = 2.02
Pt–Cl	2	5.6 (4)	2.30 (1)	R_e = 2.31
Residual = 1.5×10^{-2}, N_{par} = 5, QF = 0.75, ΔE = 5.8 (4) eV				

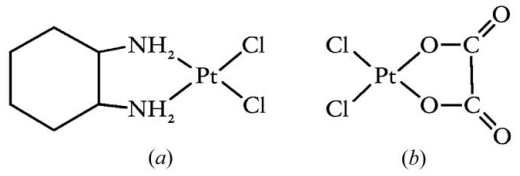

Figure 10
Model with (*a*) the diaminocyclohexane ligand and (*b*) the oxalate ligand.

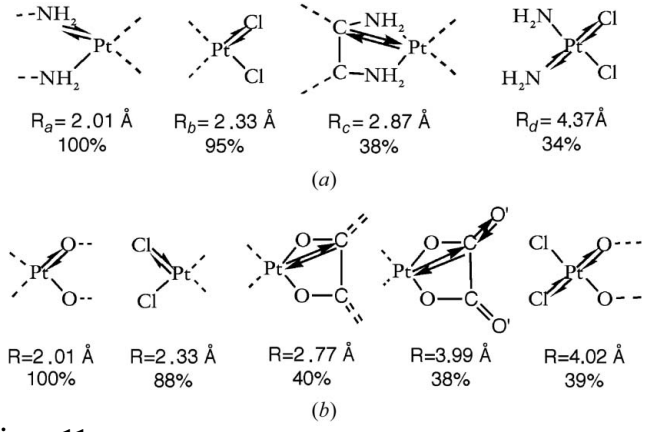

Figure 11
Most important paths in the two hypothesis: (*a*) displacement of the oxalate ligand, (*b*) displacement of the DACH ligand.

Truter, 1966; Bruck *et al.*, 1984; Beagley *et al.*, 1985; Wilson *et al.*, 1992).

It is clear from these fits that the first coordination spheres of the two degradation products by NaCl or HCl are identical. It is impossible to determine which ligand (DACH or oxalate) is displaced by these two chloride ions only by fitting the first coordination sphere. Therefore we must model the complete structure, assuming two cases: (i) model (*a*) assumes the displacement of the oxalate ligand (Fig. 10*a*); (ii) model (*b*) assumes the displacement of the DACH ligand (Fig. 10*b*). The most important paths for both models are presented in Fig. 11.

The comparison of theoretical and experimental Fourier transform (Fig. 12, for the NaCl precipitate) shows that in model (*b*) the third peak is largely overestimated. On the contrary, the whole spectrum is perfectly fitted within the error bars using model (*a*). As shown in Fig. 12(*a*), a signal of moderate amplitude remains in the experimental curve around 3.5 Å, even if the oxalato group is removed and

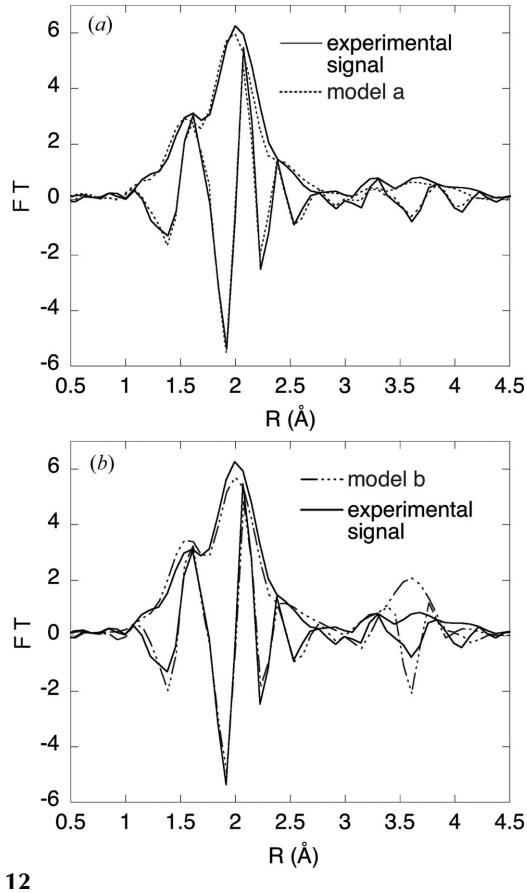

Figure 12
Comparison between the experimental signal and the two theoretical signals: model (*a*) (top) and model (*b*) (bottom).

replaced by two Cl^- ions. This contribution is correctly fitted only if we take into account the Pt–Cl–Pt–N multiple-scattering path through the central atom.

The refinement parameters for the two products of the reaction (with NaCl and HCl) are presented in Table 4. For the two compounds the F-test shows that model (*a*) (replacement of the oxalate ligand by two Cl^-) is the more likely with a probability of 95% in both cases. In this model the refined parameters are very close for both compounds. Thus we conclude that both precipitates are the [Cl_2DACH-Pt(II)] complex. It must be emphasized that the exceptional amplitude of the oxalate PtCO′ multiple-scattering contribution was the key to obtaining such a result.

4. Conclusion

The main result of this study is that oxaliplatin is degraded in [Cl_2-(DACH)-Pt(II)] in the presence of chloride ions, either in neutral or acidic media. It has been shown how EXAFS can characterize the structure of such platinum complexes. The study of oxaliplatin and its degradation products is particularly facilitated by the specific oxalate group signature, which allows an unambiguous determination of the ligand loss and of the binding of the chloride ions.

This work may help in understanding the influence of the medium on the efficiency and the toxicity of these platinum

Table 4
Comparison between the two models and parameters of the best fit for the two precipitates, and parameters of the simulations (*a*).

	Model (*a*)	Model (*b*)
NaCl precipitate		
χ^2	14.1	28.8
Number of fitted parameters	6	7
Residual	2.72×10^{-2}	5.52×10^{-2}
HCl precipitate		
χ^2	15.7	29.6
Number of fitted parameters	6	7
Residual	1.88×10^{-2}	4.55×10^{-2}

Parameters of the simulations (*a*)

Path	*N*	NaCl precipitate	HCl precipitate
R (Pt–N) (Å)	2	2.02 (1)	2.01 (1)
R (Pt–Cl) (Å)	2	2.313 (3)	2.31 (1)
R (Pt–C) (Å)	2	2.86 (2)	2.89 (1)
R (Pt–N–Pt–Cl) (Å)	2	4.34 (6)	4.35 (2)
Global $\sigma \times 10^2$ (Å)		5.6 (3)	5.8 (2)
Global ΔE (eV)		6.76 (2)	6.98 (4)

anticancer drugs. Degradation of oxaliplatin and other platinum drugs by various nucleophilic reagents are under study. Knowledge of the structures of the platinum complexes obtained under such conditions is key to these studies. With its recent improvements (multiple-scattering analysis, *ab initio* codes), EXAFS is the best alternative to X-ray diffraction when the studied complexes are poorly crystallized or still in solution.

We would like to thank Professor Simone Benazeth, and Dr Jacques Moscovici for data collection at LURE and ELETTRA and helpful discussions. Financial support from the European Community, Research Infrastructure Action under the FP6 'Structuring the European Research Area' Program (through the Integrated Infrastructure Initiative 'Integrating Activity on Synchrotron and Free Electron Laser Science') is gratefully acknowledged, as well as financial support from the French Ministry of Education. Our error analysis was largely improved by fruitful discussions with Professor Dale Sayers, who passed away last Fall. This paper is dedicated to his memory.

References

Beagley, B., Cruickshank, D. W. J., McAuliffe, C. A., Pritchard, R. G., Zaki, A. M., Beddoes, R. L., Cernik, R. J. & Mills, O. S. (1985). *J. Mol. Struct.* **130**, 97–102.
Benaji, B., Dine, T., Luyckx, M., Brunet, C., Goudaliez, F., Mallevais, M. L., Cazin, M., Gressier, B. & Cazin, J. C. (1994). *J. Clin. Pharm. Ther.* **19**, 95–100.
Bruck, M. A., Bau, R., Noji, M., Inagaki, K. & Kidani, Y. (1984). *Inorg. Chim. Acta*, **92**, 279–284.
Chollet, P., Bensmaine, M., Brienza, S., Deloche, C., Cure, H., Caillet, H. & Cvitkovic, E. (1996). *Ann. Oncol.* **7**, 1065–1070.
Curis, E., Provost, K., Bouvet, D., Nicolis, I., Crauste-Manciet, S., Brossard, D. & Benazeth, S. (2001). *J. Synchrotron Rad.* **8**, 716–718.
Curis, E., Provost, K., Nicolis, I., Bouvet, D., Benazeth, S., Crauste-Manciet, S., Brion, F. & Brossard, D. (2000). *New J. Chem.* **24**, 1003–1008.
Joyner, R. W., Martin, K. J. & Meehan, P. J. (1987). *J. Phys. C*, **20**, 4005–4012.
Koenigsberger, D. C. & Prins, R. (1988). *X-ray Absorption Principles, Applications, Techniques of EXAFS, SEXAFS and XANES.* New York: Wiley.
Lederer, M. & Leipzig-Pagani, E. (1998). *Int. J. Pharm.* **167**, 223–228.
Lokich, J. (2001). *Cancer Invest.* **19**, 756–760.
Lytle, F. W., Sayers, D. E. & Stern, E. A. (1989). *Physica B*, **158**, 701.
Mattes, V. R. & Krogmann, K. (1964). *Z. Anorg. Allg. Chem.* **332**, 247–256.
Michalowicz, A. (1997). *J. Phys. IV*, **7**(C2), 235–236.
Michalowicz, A., Provost, K., Laruelle, S., Mimouni, A. & Vlaic, G. (1999). *J. Synchrotron Rad.* **6**, 233–235.
Milburn, G. H. W. & Truter, M. R. (1966). *J. Chem. Soc. A*, pp. 1609–1616.
Provost, K., Champloy, F. & Michalowicz, A. (2001). *J. Synchrotron Rad.* **8**, 1109–1112.
Rehr, J. J., Zabinski, S. I. & Alberts, A. C. (1992). *Phys. Rev. Lett.* **69**, 3397–4000.
Rixe, O., Ortuzar, W., Alvarez, M., Parker, R., Reed, E., Paull, K. & Fojo, T. (1996). *Biochem. Pharmacol.* **52**, 1855–1865.
Sanderson, B. J. S., Ferguson, L. R. & Denny, W. A. (1996). *Mutat. Res.* **355**, 59–70.
Scheeff, E. D., Briggs, J. M. & Howell, S. B. (1999). *Mol. Pharmacol.* **56**, 633–643.
Teo, B. K. (1981). *J. Am. Chem. Soc.* **103**, 3990–4001.
Teo, B. K. (1986). *Inorganic Chemistry Concepts, EXAFS: Basic Principles and Data Analysis.* Berlin: Springer.
Valiere, C., Arnaud, P., Caroff, E., Dauphin, J. F., Clement, G. & Brion, F. (1996). *Int. J. Pharm.* **138**, 125–128.
Wilson, C., Scudder, M. L., Hambley, T. W. & Freeman, H. C. (1992). *Acta Cryst.* C**48**, 1012–1015.
Wiseman, L. R., Adkins, J. C., Plosker, G. L. & Goa, K. L. (1999). *Drugs Aging*, **14**, 459–475.